

Zero-phonon lines in the photoluminescence spectra of MgO:Mn²⁺ nanocrystals

Igor S. Altman,^{1,2} Peter V. Pikhitsa,^{1,*} Mansoo Choi,^{1,†} Ho-Jun Song,³ Albert G. Nasibulin,⁴ and Esko I. Kauppinen⁴
¹National CRI Center for Nano Particle Control, Institute of Advanced Machinery and Design, Seoul National University, Seoul 151-742, Korea

²School of Environmental Engineering, Griffith University, Brisbane, 4111 Queensland, Australia

³Chonnam National University, Gwangju 500-757, Korea

⁴VTT Processes, Aerosol Technology Group, P.O.Box 1602, FIN-02044 VTT Espoo, Finland

(Received 24 June 2003; revised manuscript received 4 August 2003; published 26 September 2003)

We report the observation of a pair of sharp zero-phonon lines in MgO:Mn²⁺ nanocrystals, which appear simultaneously in photoluminescence. We suggest a reason why these lines have not yet been observed in the system in question even in the bulk material, but appear in nanocrystals synthesized by combustion. The easiness of the excitation of extremely sharp zero-phonon lines makes our finding attractive for optical nanodevice applications.

DOI: 10.1103/PhysRevB.68.125324

PACS number(s): 78.55.Et, 78.67.Bf

I. INTRODUCTION

Over several decades, the study of crystalline lattice defects has derived a considerable impetus from the need to understand the control exerted by defects on most technologically important properties of solids. Among different types of structures investigated, MgO is in the forefront of research. Having the simplest (rock-salt) lattice structure and the large energy gap MgO is a suitable ground to test theoretical models describing properties of defects and to compare their prediction with experimental results. One of key-role defects being studied in MgO crystals is Mn²⁺,¹⁻¹² which substitutes magnesium in octahedral sites. The interest for MgO:Mn²⁺ structure is caused by both the easiness of preparation of this valence state of the manganese ion in MgO host and the clear way of its theoretical description. However, despite the long history of studies, there has been no direct observation of an excited state of Mn²⁺ ion in MgO whose energy is a subject of theoretical debates.^{9,10} Note that the excited states of Mn²⁺ in octahedral sites in some different matrices¹³⁻¹⁷ as well as the states of Mn⁴⁺ in MgO (Refs. 18-20) are known to produce sharp zero-phonon lines (ZPL's). In the present paper we report the observation of ZPL's originating from electron transitions of Mn²⁺ ion in MgO matrix. These lines were observed in macroscopic photoluminescence (PL) from nanocrystals synthesized by combustion. To our best knowledge this is the first observation of extremely sharp emission lines from nanocrystals. The simultaneous appearance of a pair of zero-phonon lines in PL from transition-metal defects as in our system has not yet been reported as well. The values of energies of observed lines allow one to choose the crystal-field strength in MgO, magnitude of which is one of the main parameters being used in the theoretical modeling.

II. EXPERIMENT

The nanocrystals of MgO were synthesized by burning out Mg particles in air as described elsewhere.^{21,22} We used Mg particles (Alfa Aesar) with size about 2-4 mm and nominal purity of 99.98%. Actually, the purity of Mg in use

[that was checked with the inductively coupled plasma analysis] was higher and the main impurity was Mn with a content of 12.8 ppmw. The MgO nanocrystals obtained after Mg particle burning were also checked with ICP to show Mn content of 2.3 ppmw. The close value (about 3 ppmw) was derived from electron-spin-resonance (ESR) spectra (see below). No other impurity was found in MgO. The synthesized MgO particles look perfect cubes [see Fig. 1(a)] with the average size about 30 nm. In the same figure the electron-diffraction pattern of the particles is presented. The electron-diffraction ring pattern simulation performed for MgO fits

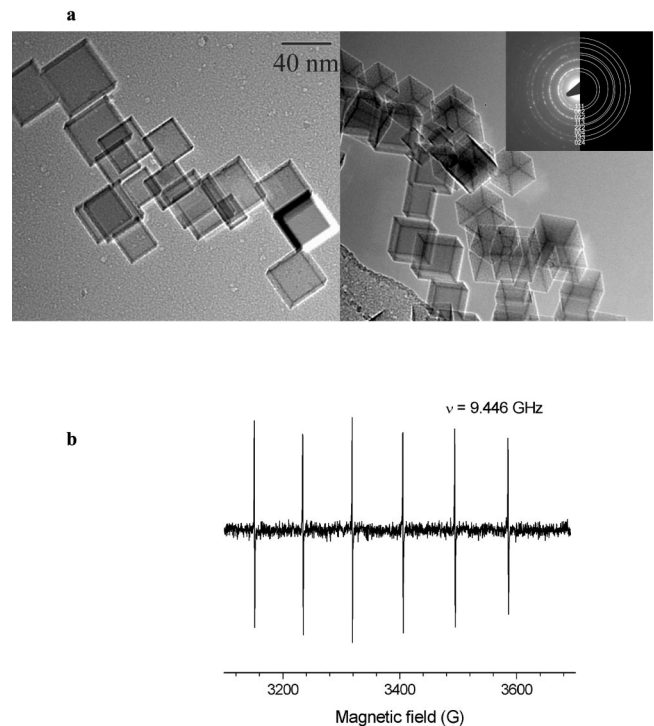


FIG. 1. Structural characteristics of MgO nanocrystals. (a) TEM images. Inset shows the electron-diffraction pattern together with the ring pattern simulation. (b) Derivative ESR spectrum of MgO nanocrystals. Sextet parameters (see text) correspond to Mn²⁺ ion in MgO host.

the experimental results demonstrating a good crystallinity of particles. X-ray-diffraction analysis also confirms it. In order to check the valence state of Mn ion in MgO particles we carried out ESR measurements at X band. We found the sextet [see Fig. 1(b)] with parameters $g=2.0016$ and $|A|=81 \times 10^{-4} \text{ cm}^{-1}$ corresponding to MgO:Mn²⁺ system¹ at both measurement temperatures (77 K and 300 K). The peak-to-peak width of components at microwave power below the ESR saturation was about 0.5 G. The narrowness of the ESR peaks together with the sextet parameters give evidence that all Mn²⁺ ions occupy cubic sites in our MgO particles. In order to measure PL MgO nanopowder was pressed into pellets. The cryostat allowed us to cool samples down to about 10 K. PL was excited by continuous-wave (cw) He-Cd ($\lambda_{exc}=325 \text{ nm}$) and Ar-ion ($\lambda_{exc}=514.5 \text{ nm}$) lasers for cw PL measurements, and by pulsed Nd:YAG (yttrium aluminum garnet) laser ($\lambda_{exc}=266 \text{ nm}$) for time-resolved photoluminescence (TRPL) measurements. The 150-W xenon lamp with a scanning monochromator was used in order to obtain photoluminescence excitation (PLE) spectra. In all the cases the excitation density did not exceed of 1 W/cm^2 . At the PL yield measurements the incident laser intensity was changed with metallic neutral density filters. The spectra were detected with a 0.85-m double monochromator (SPEX 1403) equipped with a R943-02 GaAs photomultiplier tube (for cw PL and PLE measurements) and with a 0.5-m spectrometer (Acton Research) equipped with an intensified photodiode array (1024 pixels) detector (TRPL measurements).

III. RESULTS AND DISCUSSION

The typical cw PL spectra measured at 10 K are shown in Fig. 2(a). Two sharp ZPL's are clearly seen. At 10 K the first line peaking at 659.23 nm has a full width at half maximum (FWHM) of 0.7 \AA and the second one peaking at 735.45 nm has a FWHM of 1.9 \AA . Note that unlike quantum dots (QD's) which exhibit sharp lines only in microscopic PL (Ref. 23) (in the case when emission from an individual QD is distinguished), our particles emit sharp lines in macroscopic PL (when emission from all particles come to the detector). As one can see the second ZPL (the 735-nm ZPL) is accompanied with conventional phonon replicas,^{24,25} while the first ZPL (the 659-nm ZPL) does not produce these replicas. The temperature evolution of ZPL's is shown in Figs. 2(b) and (c). The intensity of the found ZPL's strongly depends on the measurement temperature showing a temperature quenching. The line intensities vs temperature are given in Fig. 3(a). The function $1/[1 + K \exp(-E_A/T)]$ demonstrates a good fit to the experimental points. The activation energy E_A is of 360 K for the 659-nm ZPL and of 460 K for the 735-nm ZPL. The PL yield that is a dependence of ZPL intensity I upon the incident laser power P is shown in Fig. 3(b). It exhibits $I \propto P^n$ law with $n \approx 1$ (one-photon excitation). This dependence was observed for both the cw excitation and the pulsed one.

The typical spectra measured at 10 K with the 5- μsec gate at different delay times after the Nd:YAG laser excitation are shown in Fig. 4. The ZPL's broadness is caused by the low spectral resolution of the spectrometer enabling to

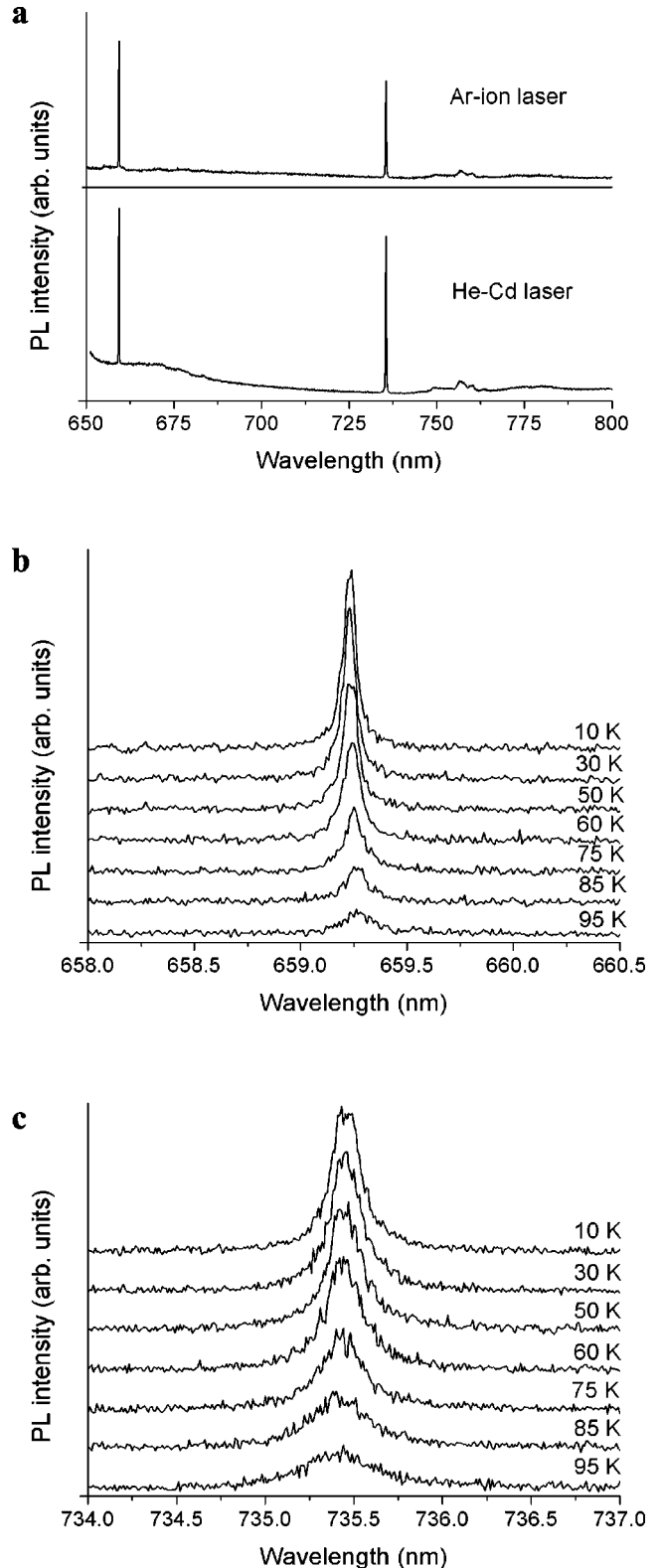


FIG. 2. cw PL spectra. (a) PL spectra excited by different lasers at 10 K. Two sharp ZPL's are clearly distinguished. (b,c) Temperature evolution of the 659-nm ZPL and the 735-nm ZPL, respectively. The spectra are offset. Measurements were done under the Ar-ion laser excitation.

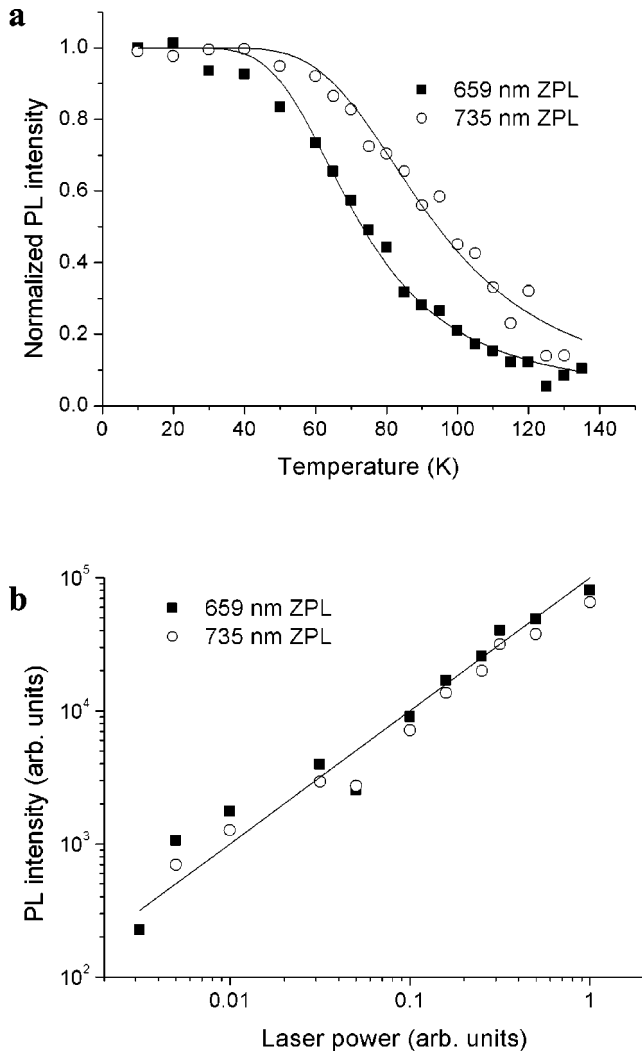


FIG. 3. Results of the ZPL's studies. (a) PL intensity of ZPL's normalized to the value at 10 K vs the temperature. Solid lines show fitting with the function $1/[1 + K \exp(-E_A/T)]$ (see text). (b) PL yield. The solid line corresponding to the $I \propto P$ dependence (one-phonon excitation) is a guide for eye.

measure TRPL at a wide region. All the spectra demonstrate similar features that correspond to the similar decay of the ZPL's and the continuous background. The decays of background luminescence at different wavelengths replotted from the TRPL spectra are shown in Fig. 5. Figure 6 demonstrates the luminescence decay of the ZPL's. As one can see both the background and the ZPL's show the characteristic luminescence decay time of 0.1 msec, though the background also experiences an initial fast decay.

In order to obtain the bare PLE spectra of the ZPL's we took the PLE spectra for emission exactly at the ZPL's wavelengths and at the wavelengths shifted from the ZPL's on 1–2 nm. The PLE spectrum at the wavelength close (but not coinciding) to a ZPL can be considered as the PLE spectrum of the background at the ZPL wavelength. Then the difference between the PLE spectra at the ZPL's wavelength and at those close to the ZPL's gives the bare PLE spectra of the ZPL's. These bare PLE spectra of the ZPL's obtained at 10 K

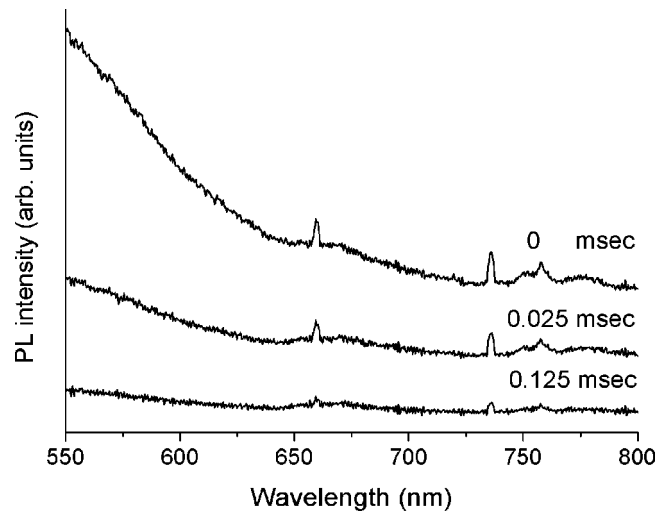


FIG. 4. PL spectra at 10 K corresponding to different delay times after the Nd:YAG laser excitation. The spectra are offset. The ZPL's broadness is caused by the low spectral resolution of the spectrometer enabling us to measure TRPL at a wide region.

are shown in Fig. 7. Note that the relatively high noise in the PLE spectra is caused by the weakness of PL under the scanned xenon lamp excitation. Nevertheless, the similarity of the bare PLE spectra of both ZPL's can be concluded. The PLE spectra show that ZPL's can be excited in a wide energy range. The latter corresponds to the ZPL's observation under excitation with different lasers covering a broad range (laser wavelengths of 266 nm, 325 nm, and 514.5 nm). At room temperature no bare PLE spectra were found.

Let us analyze the experimental results. The ZPL's come from a forbidden electric dipole transition. This is typical for transition-metal ions.^{24,25} Based on the result of ESR measurements the transition-metal ion in our case is Mn^{2+} in MgO matrix. For such a Mn^{2+} ion in an octahedral environment other than MgO only one ZPL in luminescence is usually observed. Such ZPL corresponds to the transition from

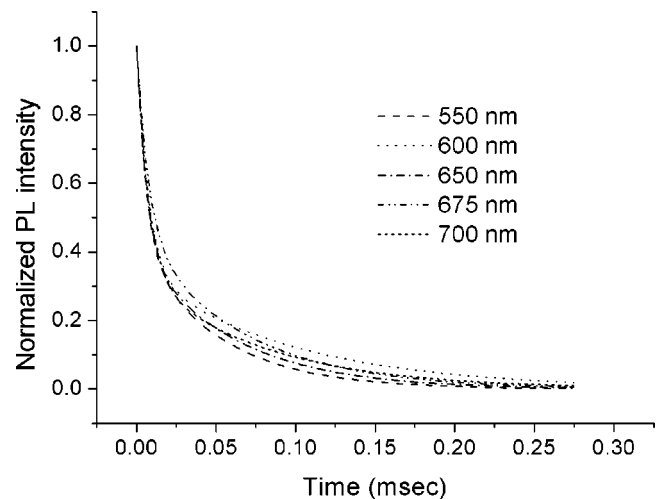


FIG. 5. Decay of background luminescence at different wavelengths after the Nd:YAG laser excitation at 10 K. Intensities are normalized to initial values.

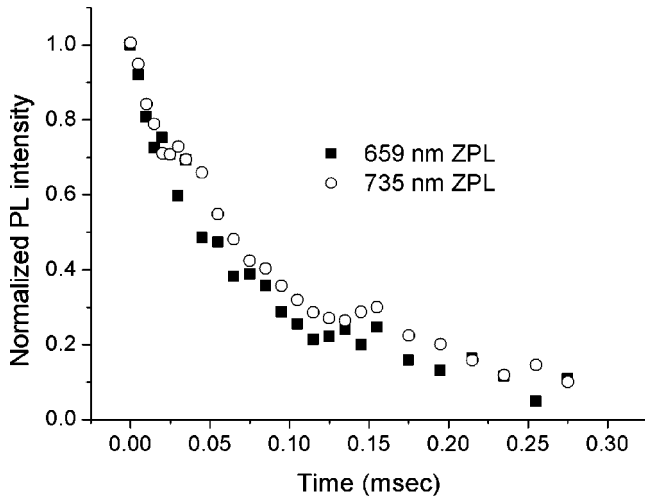


FIG. 6. Decay of ZPL's luminescence after the Nd:YAG laser excitation at 10 K. Intensities are normalized to initial values.

the lowest excited ${}^4T_1({}^4G)$ state to the ground ${}^6A_1({}^6S)$ state. Other excited states decay by the nonradiative relaxation dropping onto the lowest excited state and PL from all excited states except the lowest one is suppressed.²⁴ The appearance of two ZPL's in our system indicates that there is an excited state, which does not decay by the nonradiative transition. It may be possible if this state is weakly coupled with phonons. Then a lack of phonon replicas for the 659-nm ZPL becomes clear. At the same time the ${}^4T_1({}^4G)$ - ${}^6A_1({}^6S)$ transition is characterized by a large value of the Huang-Rhys parameter^{24,25} giving the pronounced phonon replicas of the 735-nm ZPL. In order to confirm that both ZPL's observed in the PL really belong to Mn we additionally measured PL from nanocrystals with different Mn content. Such nanocrystals were produced by burning out Mg particles at the presence of Mn-containing salt (MnCl_2). For all impurity levels checked (up to a few hundred ppmw) intensities of both ZPL's increased with the Mn content increase. The ratio of intensities remained constant, which allows one to claim that

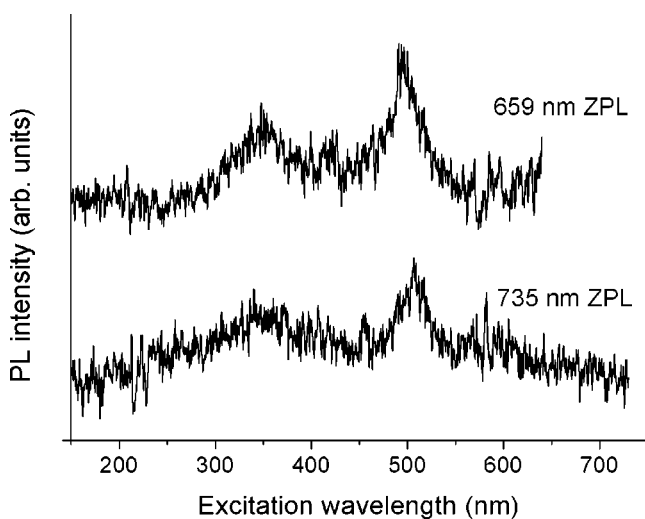


FIG. 7. Bare PLE spectra of ZPL's taken at 10 K. The spectra are offset.

the same center of impurity is responsible for the found ZPL's. Also we produced $\text{MgO}:\text{Cr}^{3+}$ nanocrystals that exhibited sharp lines at 698.07 nm (*R* line) and at 703.79 nm (*N* line). This wavelength exactly coincide with that reported for bulk $\text{MgO}:\text{Cr}^{3+}$ system.^{26,27} The absence of Cr^{3+} -originating lines in MgO nanocrystals different from those in the bulk matrix confirms the absence of the specific nanocrystal sites occupied by substituted ions, existence of which might be brought into question in order to explain the origin of ZPL's in the $\text{MgO}:\text{Mn}^{2+}$ system. The latter shows that the finite size of our MgO nanocrystals does not affect the energy levels of a substituted ion.

We have to emphasize that despite many years of $\text{MgO}:\text{Mn}^{2+}$ study, ZPL's have not been reported previously even for bulk neither in emission nor in absorption. Then the exact values of energy levels of Mn^{2+} ion in octahedral sites of MgO have not been known for such (probably the simplest) transition ion crystalline matrix system.

Let us assign the 659-nm ZPL for a transition by using the Tanabe-Sugano diagram for the $3d^5$ system.^{28,29} As we noted before the 735 ZPL undoubtedly comes from the $T_1({}^4G)$ - ${}^6A_1({}^6S)$ transition. The energy of this transition corresponds to $Dq/B \sim 1.5$, where Dq is the crystal-field strength and B is the Racah parameter. Note that such a large value of Dq/B corresponds to latest calculations.¹¹ At so high a value of Dq/B the next state ${}^4T_2({}^4G)$ coming from splitting of the 4G term in the crystal field lies at about 5000 cm^{-1} higher than the ${}^4T_1({}^4G)$ state. Since the energy difference between ${}^4T_2({}^4G)$ and ${}^4T_1({}^4G)$ states is more than three times larger compared to the distance between two observed ZPL's, the 659 nm ZPL cannot come from the ${}^4T_2({}^4G)$ - ${}^6A_1({}^6S)$ transition. At the same time the large energy separation between two ZPL's observed (about 1500 cm^{-1}) does not allow one to assign the 659-nm ZPL for the $T_1({}^4G)$ - ${}^6A_1({}^6S)$ transition of Mn^{2+} ion in a site other than the octahedral one as far as the 735-nm ZPL is assigned to the $T_1({}^4G)$ - ${}^6A_1({}^6S)$ transition of Mn^{2+} ion in the octahedral site. However, at $Dq/B \sim 1.5$ a state coming from splitting of the 2I term appears within the needed energy region and matches observation. We claim that just the transition from this state to the ground ${}^6A_1({}^6S)$ state gives the 659-nm ZPL. Then, because states from different electron terms are responsible for two observed ZPL's two essentially different Huang-Rhys parameters may correspond to the transitions. It leads to the absence of phonon replicas for the 659-nm ZPL (which is likely weakly coupled with phonons) and the existence of them for the 735-nm ZPL. Note that the idea similar to ours, which uses 2I term in order to match the experimental data to the Tanabe-Sugano diagram was previously applied to $\text{ZnS}:\text{Mn}^{2+}$ system.¹³ The authors¹³ also discussed how so strongly forbidden free-ion transition between the ground state 6S and the 2I level becomes allowed in the presence of the crystalline field. Note once again that although the above idea utilizing 2I term in order to explain the origin of the 659-nm ZPL looks unconventional, it is the only way to explain so unforeseen a fact as an appearance of the second ZPL originating from the same transition ion in the matrix (which to our best knowledge has not been observed previously).

As one can see in Fig. 6 both ZPL's exhibit a similar luminescence time decay. It seems to be difficult to explain how the lines arising from different spin manifolds can have the same lifetimes. Even transitions originating from the same level of ions occupying different sites should have different lifetimes. Then we have to conclude that the luminescence decay shown in Fig. 6 has nothing to do with the pure radiative lifetimes of emitting states (which can be sufficiently short in nanocrystals^{30,31}) and the luminescence decay time likely corresponds to the time decay of states exciting ZPL's. If the ZPL's are excited from the same states (see below), then the similarity of the time decay for both ZPL's becomes clear. The decay of background luminescence similar to the ZPL's decay (see Figs. 4–6) gives an evidence that the long-time background luminescence is excited by the same mechanism as the ZPL's are (from the same states). Note that the fast decaying part of the background luminescence (lying beyond the present work) may be attributed to the luminescence of F centers.³²

The next question that should be discussed is why ZPL's found in the present paper have not been observed previously, despite numerous studies of the MgO PL. The answer to this question is important in order to understand our finding. Note that ZPL's originating from Mn^{2+} transitions in cubic crystalline field were seen before only in PL of narrow-band materials. The thermal quenching and the PL yield observed in the present paper for ZPL's are similar to those for the PL, when the emitting states are excited from some close electron states. For such a wide-gap substance as is MgO these states should lie deep inside the forbidden band and therefore cannot exist in ordinary MgO crystals. Then the energy transfer between the environment and excited states of Mn^{2+} ion does not occur making the Mn^{2+} ion excitation

impossible. It explains why in usual MgO crystals ZPL's were not observed. Note that if nanoparticles are generated by vapor condensation during combustion, a high concentration of structural defects in particle substance takes place.^{33,34} It appears due to the fast rate of particle formation and exhibits itself via anomalously high light absorption found in our recent studies of wide-gap nanooxides.^{21,22,33,34} Just the presence of these defects, which is a distinctive feature of particles synthesized by combustion, leads to the existence of states deep inside the forbidden band and to the possibility to excite a Mn^{2+} ion in MgO matrix and therefore to the appearance of the Mn^{2+} -originating ZPL's in PL. This idea of the ZPL's excitation corresponds to the observed similarity of the PLE spectra (see Fig. 7), which give the information about the density of states exciting the ZPL's. It should be added that the easiness of the excitation of the Cr^{3+} -originating ZPL's even in bulk is related to a specific charge state of the Cr^{3+} ion which itself is a defect in the MgO matrix.

The present paper demonstrates that combustion nanooxides give way to excite perfect ZPL's from them unlike nanocrystals synthesized in another way.³⁵ We believe that the combustion nanocrystals can be utilized in optical nanodevices due to extraordinary discreteness of the system energy levels with the performance better than that of QD's.

ACKNOWLEDGMENTS

The authors thank J. E. Yi at Korea Basic Science Institute for assistance in measurements. Fruitful discussions with B. Henderson are gratefully appreciated. This work was funded by the Creative Research Initiatives Program supported by the Ministry of Science and Technology, Korea. A.G.N. and E.I.K. acknowledge support from TEKES, Finland.

*On leave from Physics Institute, Odessa National University, Odessa, Ukraine.

†Corresponding author. Email address: mchoi@plaza.snu.ac.kr

¹W. Low, Phys. Rev. **105**, 793 (1957).

²H. Watanabe, Phys. Rev. Lett. **4**, 410 (1960).

³M.J.D. Powell, J.R. Gabriel, and D.F. Johnston, Phys. Rev. Lett. **5**, 145 (1960).

⁴W.M. Walsh, Jr., Phys. Rev. **122**, 762 (1961).

⁵E.R. Feher, Phys. Rev. **136**, A145 (1964).

⁶P.R. Solomon, Phys. Rev. **152**, 452 (1966).

⁷P. Koidl and K.W. Blazey, J. Phys. C **9**, L167 (1976).

⁸J.O. Rubio, E.P. Muñoz, J.O. Boldú, Y. Chen, and M.M. Abraham, J. Chem. Phys. **70**, 633 (1979).

⁹Du Mao-Lu and Zhao Min-Guang, J. Phys. C **18**, 3241 (1985).

¹⁰Kuang Xiao-Yu, Phys. Rev. B **37**, 9719 (1988).

¹¹Yu Wan-Lun, Phys. Rev. B **39**, 622 (1989).

¹²B.L. Gordon and M.S. Seehra, Phys. Rev. B **40**, 2348 (1989).

¹³D. Langer and S. Ibuki, Phys. Rev. **138**, A809 (1965).

¹⁴D.W. Langer and H.J. Richter, Phys. Rev. **146**, 554 (1966).

¹⁵R.L. Greene, D.D. Sell, R.S. Feigelson, G.F. Imbusch, and H.J. Guggenheim, Phys. Rev. **171**, 600 (1968).

¹⁶F. Bantien and J. Weber, Phys. Rev. B **37**, 10 111 (1988).

¹⁷N. Yamashita and A. Takagoshi, Jpn. J. Appl. Phys., Part 1 **36**, 5532 (1997).

¹⁸J.S. Prener, J. Chem. Phys. **21**, 160 (1953).

¹⁹B. Henderson and T.P.P. Hall, Proc. Phys. Soc. London **90**, 511 (1967).

²⁰K. Dunphy and W.W. Duley, J. Phys. Chem. Solids **51**, 1077 (1990).

²¹Yu. L. Shoshin and I.S. Altman, in *Combustion of Energetic Materials*, edited by K.K. Kuo and L.T. De Luca (Begell House, New York, 2002), p. 773.

²²Yu.L. Shoshin and I.S. Altman, Combust. Sci. Technol. **174**, 209 (2002).

²³M. Notomi, T. Furuta, H. Kamada, J. Temmyo, and T. Tamamura, Phys. Rev. B **53**, 15 743 (1996).

²⁴G.F. Imbusch and R. Kopelman, in *Laser Spectroscopy of Solids* edited by W.M. Yen and P.M. Selzer (Springer-Verlag, Berlin, 1981), p. 1.

²⁵B. Henderson and G.F. Imbusch, *Optical Spectroscopy of Inorganic Solids* (Clarendon, Oxford, 1989).

²⁶G.F. Imbusch, W.M. Yen, A.L. Schawlow, D.E. McCumber, and M.D. Sturge, Phys. Rev. **133**, A1029 (1964).

²⁷J.P. Larkin, G.F. Imbusch, and F. Dravnieks, Phys. Rev. B **7**, 495 (1973).

²⁸Y. Tanabe and S. Sugano, J. Phys. Soc. Jpn. **9**, 766 (1954).

²⁹E. König and S. Kremer, *Ligand Field Energy Diagrams* (Plenum, New York, 1977).

- ³⁰K. Yan, C. Duan, Y. Ma, S. Xia, and J.-C. Krupa, *Phys. Rev. B* **58**, 13 585 (1998).
- ³¹B.A. Smith, J.Z. Zhang, A. Joly, and J. Liu, *Phys. Rev. B* **62**, 2021 (2000).
- ³²G.H. Rosenblatt, M.W. Rowe, G.P. Williams, Jr., R.T. Williams, *Phys. Rev. B* **39**, 10 309 (1989).
- ³³I.S. Altman, D. Lee, J.D. Chung, J. Song, and M. Choi, *Phys. Rev. B* **63**, 161402 (2001).
- ³⁴P.V. Pikhitsa and I.S. Altman, *J. Nanopart. Res.* **3**, 303 (2001).
- ³⁵S.V. Bulyarskii, A.E. Kozhevnikov, S.N. Mikov, and V.V. Prikhodko, *Phys. Status Solidi A* **180**, 555 (2000).